

To aid in the use of band contours in vibrational assignments Ueda and Shimanouchi³¹ computed the typical type A, B, and C contours for 40 different sets of constants with the assumption that they did not change with vibrational excitation. While the contours differed in their details depending upon the individual constants, one could generally recognize the band types by comparison with typical contours such as those shown in Figure 3a-c, except in extreme cases when the molecule is very close to an exact symmetrical top limit. In the case of pyridine-*d*₅ we have found that the effective rotational constants can change sufficiently with vibrational excitation to completely change the apparent band type. While the generality of this observation awaits high-resolution, band contour analysis of other systems, this investigation raises questions concerning the validity of using simple band contour arguments in the determination of vibrational assignments. When the effect of vibrational excitation on the rotational constants is sufficiently large, the observed contour may be completely opposite to that which is expected. Thus, observed band contours can be misleading and must be applied to vibrational analyses with caution.

Besides the ν_{6a} band of pyridine-*d*₅, the high-resolution spectra of pyridine, pyridine-*d*₅, and pyridine-4-*d* contain many other interesting and, in some cases, inexplicable features. One example is a pyridine-4-*d* band at about 860

cm⁻¹, which was assigned by Wilmschurst and Bernstein⁵ as simultaneously belonging to two *b*₁ and one *b*₂ fundamental vibrations. Under 0.07-cm⁻¹ resolution it is a broad continuum containing three major maxima with weak but well-defined underlying rotational structure. At this resolution the observed band contour is unlike any "typical" contour although it was assigned to a type C contour at much lower resolution.^{5,13} Another interesting observation is that some bands possess sharp and well-defined rotational structure (such as the ν_{6a} band of pyridine-*d*₅) while others appear to be structureless (in a relative sense). In some but not all cases this may be due to strong overlapping bands. The computational experience gained in this work shows that a structureless band is generally related to large changes (say 1%) in rotational constants. This further *calls into question* the use of typical band contour shapes as a method for assigning the bands in the infrared spectrum of pyridine as such large changes in the rotational constants can completely change the overall shape of the contour.

Acknowledgment. The authors are grateful to the National Science Foundation (Grant CHE8017304) for their support of this research. K.N.W. also expresses his gratitude to Mr. R. Dempsey and Miss D. Snively for their assistance with the band contour calculations and to Dr. M. Seaver for many helpful discussions.

Registry No. Pyridine-*d*₅, 7291-22-7.

(31) T. Ueda and T. Shimanouchi, *J. Mol. Spectrosc.*, **28**, 350 (1968).

Librational Motion of Hexahydro-1,3,5-trinitro-*s*-triazine Based on the Temperature Dependence of the Nitrogen-14 Nuclear Quadrupole Resonance Spectra: The Relationship to Condensed-Phase Thermal Decomposition

R. J. Karpowicz and T. B. Brill*

Department of Chemistry, University of Delaware, Newark, Delaware 19711 (Received: October 4, 1982)

The intermolecular cohesive interactions in hexahydro-1,3,5-trinitro-*s*-triazine, C₃H₆N₆O₆, known as RDX, are analyzed and contrasted with those of the closely related HMX molecule, C₄H₈N₈O₈. HMX and RDX are telomers of methylenenitramine. Unlike HMX, the crystal lattice of RDX has no important O...C attractions and is dominated by O...N and N...N attractions. The temperature dependence of the ¹⁴N NQR coupling constants was measured with a pulse FT NQR spectrometer. The temperature coefficients are at least twice as large in RDX as they are in HMX, which indicates that a greater amount of librational motion and a lesser amount of intermolecular cohesion exists in RDX. The results suggest that the intermolecular forces are less important in the condensed-phase thermal decomposition of RDX than for HMX.

Introduction

Hexahydro-1,3,5-trinitro-*s*-triazine (RDX), the cyclic trimer of methylenenitramine, is one of the more important energetic compounds. Its structure is shown in Figure 1. Considerable interest exists in the molecular dynamics and thermal properties of RDX as well as in the closely related cyclic tetramer of methylenenitramine, known as HMX.^{1,2}

We have characterized the molecular dynamics of HMX in the solid phase as a function of temperature^{3,4} and pressure.^{5,6} An important finding is the similarity of the activation energy barriers for the solid-solid phase transitions in HMX to those for the condensed-phase thermal decomposition.⁴ The coincidence suggests that strong intermolecular cohesive forces largely control the rate of thermal decomposition of HMX in the condensed phase.

(1) Shaw, R.; Walker, F. E. *J. Phys. Chem.* **1977**, *81*, 2572.

(2) McCarty, K. P. AFRPL-TR-76-59, Air Force Rocket Propulsion Laboratory, Edwards AFB, CA, 1976. Schroeder, M. A., CIPA Publ. 308, Vol. II, pp 17-34, Sept. 1979. CIPA Publ. 329, Vol. II, pp 498-508, Sept. 1980. CIPA Publ. 347, Vol. II, pp 395-413, Oct. 1981.

(3) Landers, A. G.; Brill, T. B.; Marino, R. A. *J. Phys. Chem.* **1981**, *85*, 2618.

(4) Brill, T. B.; Karpowicz, R. J. *J. Phys. Chem.* **1982**, *86*, 4260.

(5) Landers, A. G.; Brill, T. B. *J. Phys. Chem.* **1980**, *84*, 3573.

(6) Karpowicz, R. J.; Brill, T. B. *AIAA J.* **1982**, *20*, 1586.

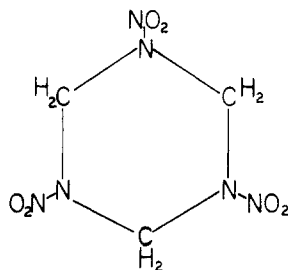


Figure 1. Structure of the RDX molecule.

Because HMX and RDX are closely related chemically, it is important to determine whether the intermolecular forces of RDX also control the rate of thermal decomposition of RDX in the condensed phase. Unfortunately, first-order thermally induced solid-solid phase transitions have not been observed in RDX and so phase transition kinetics cannot be used to elucidate its intermolecular cohesion. Instead, an indication of the relative amount of intermolecular interaction was obtained from the temperature dependence of the ^{14}N nuclear quadrupole resonance (NQR) frequencies.⁷ Comparison of the results for RDX and HMX reveal that the intermolecular cohesive forces are weaker in RDX and should have less influence on the rate of thermal decomposition in the condensed phase.

Experimental Section

The nuclear quadrupole resonance spectra were observed with a Matec pulse spectrometer interfaced to a Nicolet 1180 data acquisition system. Heat-resistant high-Q NQR coils were constructed by wrapping Cu wire around a cylindrical sample vial and coating the coil with epoxy to maintain the rigidity of the coil throughout the temperature range studied. The coil was mounted in an Al can. An iron-constantan thermocouple was placed directly into the sample vial, and the digital thermometer used for temperature measurements was grounded to prevent rf pickup.

For the frequency measurements below room temperature, the sample of RDX with a particle size of 300 μm was allowed to equilibrate in slush baths made from either CO_2 or liquid N_2 and an appropriate solvent.⁸ The temperature was maintained to approximately ± 1 K. The NQR spectra were obtained by Fourier transforming the FID after 100–6000 pulses. The carrier frequency was set 2–6-kHz off-resonance. To ensure that the frequency measurements were accurate, the carrier frequency was changed and the measurements were repeated several times. The frequencies reported in Table I are accurate to within ± 1 kHz.

For temperature measurements above 328 K, the sample was immersed in a 2-L Dewar flask filled with silicone oil. A mechanical stirrer prevented gradients in the bath. A Therm-o-watch Model L-6 temperature controller was used for temperature regulation. The NQR frequency was measured as described above, or by directly matching the NQR signal to the carrier frequency.

Discussion

The RDX Lattice. The crystal lattice of RDX is built with pairs of inverted interlocked RDX⁹ as shown in Figure 2. Intermolecular electrostatic interactions are important because of the alternating relative positive and negative

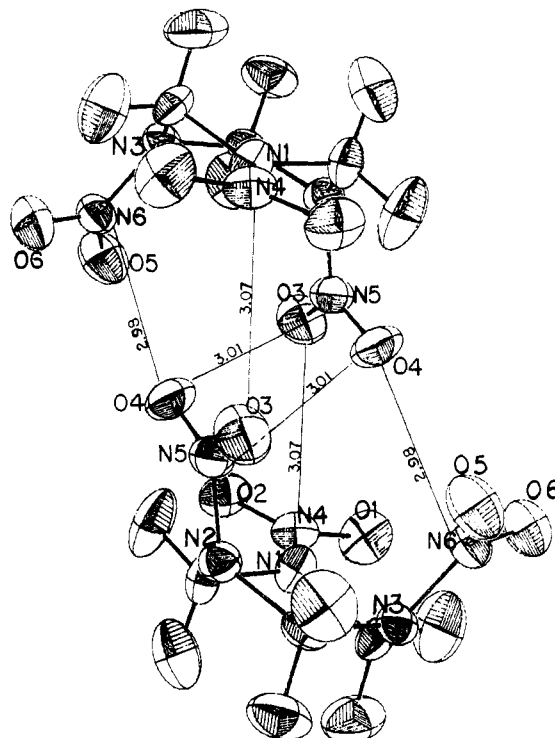


Figure 2. The "pairs" of RDX molecules and contact distances within the pairs.

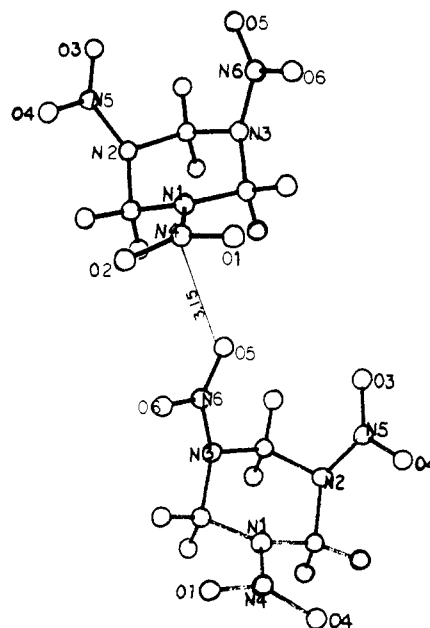


Figure 3. A major interaction occurring in the crystal lattice which holds the RDX "pairs" shown in Figure 2 together.

charges on the atoms comprising RDX. The oxygen atoms and amine nitrogen atoms are relatively negative while the carbon atoms and nitro nitrogen atoms carry relative positive charges.¹⁰ O_3 and O_4 situate in the molecular "pocket" of the neighboring molecule and attractively interact with all three nitrogen atoms of the nitro groups. Their affinity is important in holding the pairs together. O_5 attracts neighboring pairs of molecules by the interaction shown in Figure 3, such that cohesion results between all of the RDX pairs. Overall, the NO_2 group containing O_1 and O_2 engages in fewer interactions with its

(7) McEnnan, M. M.; Schempp, E. J. *J. Magn. Reson.* 1975, 11, 28.

(8) Gordon, A. J.; Ford, R. A. "The Chemist's Companion"; Wiley: New York, 1972; p 451.

(9) Choi, C. S.; Prince, E. *Acta Crystallogr., Sect. B* 1972, 28, 2857.

(10) Orloff, M. K.; Mullen, P. A.; Rauch, F. C. *J. Phys. Chem.* 1970, 74, 2189.

TABLE I: ^{14}N NQR Data for the Amine Nitrogen Atoms of RDX

T, K	ν_+ , kHz	ν_- , kHz	e^2Qq/h , kHz	η	T, K	ν_+ , kHz	ν_- , kHz	e^2Qq/h , kHz	η
77 ^a	5319	3512	5887	0.6139	278	5249	3463	5808	0.6150
	5256	3414	5780	0.6374		5199	3411	5740	0.6230
	5118	3394	5675	0.6076		5055	3364	5613	0.6026
147 ^b	5301	3499	5867	0.6143	286	5245	3462	5805	0.6143
	5242	3414	5771	0.6335		5197	3411	5739	0.6224
	5103	3388	5661	0.6059		5052	3362	5609	0.6026
176	5291	3493	5856	0.6141	298 ^c	5240	3458	5799	0.6146
	5235	3414	5766	0.6316		5192	3410	5735	0.6215
	5094	3384	5652	0.6051		5047	3359	5604	0.6024
187	5286	3490	5851	0.6139	303	5238	3457	5797	0.6145
	5231	3414	5763	0.6305		5189	3409	5732	0.6211
	5090	3383	5649	0.6044		5044	3357	5601	0.6024
200	5282	3487	5846	0.6141	308	5234	3455	5793	0.6142
	5228	3414	5761	0.6297		5187	3409	5731	0.6205
	5086	3380	5644	0.6045		5043	3355	5599	0.6030
213	5278	3483	5841	0.6147	313	5233	3453	5791	0.6148
	5224	3414	5759	0.6286		5185	3409	5729	0.6200
	5083	3378	5641	0.6045		5041	3354	5597	0.6029
228	5271	3479	5833	0.6144	318	5230	3452	5788	0.6144
	5218	3413	5754	0.6274		5183	3408	5727	0.6194
	5076	3375	5634	0.6038		5037	3353	5593	0.6021
243	5266	3476	5828	0.6143	323	5227	3450	5785	0.6144
	5214	3413	5751	0.6263		5180	3408	5725	0.6198
	5071	3373	5629	0.6033		5035	3352	5591	0.6020
250	5263	3472	5823	0.6151	328	5224	3448	5781	0.6144
	5212	3413	5750	0.6257		5178	3407	5723	0.6184
	5068	3370	5625	0.6037		5033	3349	5588	0.6027
262	5257	3470	5818	0.6143	333	5222	3447	5779	0.6143
	5207	3412	5746	0.6248		5175	3406	5721	0.6187
	5063	3368	5621	0.6031		5030	3348	5585	0.6023
273	5252	3466	5812	0.6146	338	5217	3445	5775	0.6137
	5202	3412	5743	0.6234		5173	3406	5719	0.6179
	5059	3365	5616	0.6033		5028	3346	5583	0.6026

^a ν_d observed at 1807, 1843, and 1724 kHz. ^b ν_d observed at 1802, 1827, and 1715 kHz. ^c ν_d observed at 1782 and 1688 kHz.

neighbors than do the other two NO_2 groups. It is perhaps noteworthy that the $\text{N}_1\text{--N}_4$ bond involving this NO_2 group is significantly longer than $\text{N}_2\text{--N}_5$ and $\text{N}_3\text{--N}_6$.⁹

Despite their molecular similarity, the intermolecular attractions in HMX and RDX involve somewhat different atom contacts. The attractive interactions between RDX molecules are mostly $\text{O}\cdots\text{N}$ with a few $\text{N}\cdots\text{N}$ contacts. This contrasts with HMX, where $\text{O}\cdots\text{C}$ interactions dominate the cohesion in the solid.¹¹ RDX has no important $\text{O}\cdots\text{C}$ attractions. Furthermore, one of the three NO_2 groups in RDX engages in fewer intermolecular contacts than do the other two, while in HMX all four NO_2 groups participate in numerous intermolecular interactions.

NQR Analysis. The ^{14}N NQR data for the amine nitrogen atoms of RDX are compiled in Table I. The three atoms produce a total of nine resonances corresponding to the $\nu_+(m_I = +1 \leftrightarrow 0)$, $\nu_-(m_I = -1 \leftrightarrow 0)$, and $\nu_d(m_I = +1 \leftrightarrow -1)$ transitions for each type of nucleus. The coupling constant, e^2Qq/h , and the electric field gradient asymmetry parameter, η , are computed from eq 1 and 2.¹² The

$$e^2Qq/h = 2/3(\nu_+ + \nu_-) \quad (1)$$

$$\eta = 3(\nu_+ - \nu_-)/(\nu_+ + \nu_-) \quad (2)$$

coupling constant measures the magnitude of the largest component of the electric field gradient tensor, q_{zz} , which, by convention, determines the Z principal axis. η quan-

tifies the departure of the electric field gradient from axial symmetry. The Z principal axis of the amine nitrogen is approximately perpendicular to the crude plane formed by the C_2N_2 framework, while the X and Y axes lie essentially in the plane.^{3,13-16}

A partially satisfactory interpretation of the bonding based on the Townes-Dailey formalism has been presented for HMX and RDX.³ Two of the three N--N bond distances are similar (1.35 Å) in RDX, while a third is appreciably longer (1.38 Å).⁹ Owing to the differences in the orbital populations, this variation in the bond lengths should appear clearly in the magnitude of the ^{14}N coupling constants. However, at 77 K none of the three coupling constants is unusual; the three values are about equally spaced between 5680 and 5880 KHz. This result, when linked with the fact that a Townes-Dailey analysis is only partly successful in explaining the differences between the HMX and RDX NQR data, suggests that the assignment of the three coupling constants to specific nitrogen atoms is not feasible based on Townes-Dailey theory alone. On the other hand, the temperature dependences of the coupling constants aid in assigning the values to specific nitrogen atoms.

The temperature dependence of the coupling constant originates in the librational motions, θ_i , of the molecule

(11) Brill, T. B.; Reese, C. O. *J. Phys. Chem.* **1980**, *84*, 1376.

(12) Guibe, L. *Fortschr. Chem. Forsch.* **1972**, *30*, 77.

(13) Minematsu, M. *J. Phys. Soc. Jpn.* **1959**, *14*, 1030.

(14) Smith, D. H.; Cotts, R. M. *J. Chem. Phys.* **1964**, *41*, 2403.

(15) Schempp, E.; Bray, P. J. "Physical Chemistry: An Advanced Treatise"; Academic Press: New York, 1970; Vol. 4, p 521.

(16) Subbarao, S. M.; Bray, P. J. *J. Chem. Phys.* **1977**, *67*, 1085.

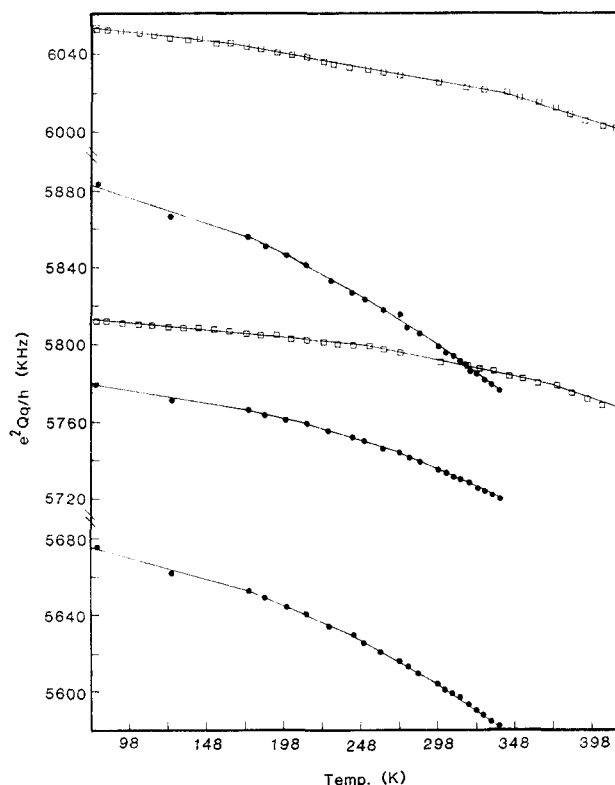


Figure 4. The temperature dependence of the ^{14}N coupling constants for the three crystallographically different amine nitrogen atoms in RDX (solid circles) and the two crystallographically different amine atoms in HMX (open squares).

about the X , Y , and Z electric field gradient axes. Equation 3 expresses the coupling constant in terms of torsional oscillations, while eq 4 gives the dependence of

$$e^2Qq/h = (e^2Qq_0/h) [1 - 3/2(\langle\theta_x^2\rangle + \langle\theta_y^2\rangle) + \eta/2(\langle\theta_y^2\rangle - \langle\theta_x^2\rangle)] \quad (3)$$

$$\langle\theta_i^2\rangle = \frac{h}{4\pi^2 I_i \nu_i} \left[\frac{1}{2} + \frac{1}{\exp(h\nu_i/kT) - 1} \right] \quad i = x, y, z \quad (4)$$

θ on temperature according to an Einstein model.¹⁷ ν_i is the i th librational frequency and I_i is the effective moment of inertia about the i th axis. The inertial axes do not coincide with the electric field gradient axes in RDX and so eq 3 only qualitatively analyzes the sensitivity of the coupling constant to temperature. It can be seen from eq 3 that the librational motions about the Z electric field gradient axis, which is perpendicular to the C_2N_2 atom plane, will hardly affect the coupling constant, while motion about the X and Y axes causes e^2Qq/h to decrease with increasing temperature.

From the rigid body model of thermal motion in RDX extracted from neutron diffraction data, Choi and Prince⁹ suggested that the largest principal axis of motion lies on the pseudo-mirror plane of the RDX molecule and makes an angle of 34° with the $\text{N}_1\text{--N}_4$ bond axis. On this basis, two of the amine nitrogen atoms should have similar temperature coefficients while the third should be unique. Moreover, by considering the librational motion with Buchi molecular models, it seems likely that the two similar

TABLE II: Temperature Coefficients for the Amine Nitrogen Atoms of RDX and HMX

RDX temp range, K	$d(e^2Qq/h)/dT$, ^a Hz/K		
	N_1	N_2	N_3
77-147	-0.129	-0.200	-0.207
176-228	-0.216 (-0.988)	-0.340 (-0.994)	-0.432 (-0.998)
243-298	-0.300 (-0.995)	-0.453 (-0.998)	-0.524 (-0.997)
303-338	-0.383 (-0.998)	-0.536 (-0.998)	-0.612 (-0.998)
HMX ² temp range, K			
	equatorial	axial	
77-270	-0.085	-0.127	
270-370	-0.181	-0.158	

^a Parenthetical numbers are the coefficients of correlation in the temperature ranges given.

amine nitrogen atoms will have somewhat larger temperature coefficients than the unique nitrogen. Their motion involves the X and Y electric field gradient axes more than does the unique nitrogen atom.

The coupling constants vs. temperature in RDX and HMX are plotted in Figure 4. Consistent with expectation from the above molecular libration analysis, one of the coupling constants possesses a smaller temperature coefficient than do the other two. This unique resonance is assignable to N_1 . The other two resonances arise from N_3 and N_5 , but cannot be distinguished by their temperature coefficients. The spread of the resonances over 200 kHz probably results from a complex blend of intermolecular and compensating intramolecular electronic effects. Further detailed conclusions are beyond the information presently at hand.

The most informative practical feature of the temperature dependence of the coupling constants lies in the comparison between RDX and HMX. The average values of $d(e^2Qq/h)/dT$ for several temperature ranges are given in Table II. On balance, the temperature coefficients are at least twice as large in RDX as they are in HMX. From this result we conclude that *the overall intermolecular cohesive force which acts to restrict librational motions of the molecule in the solid is less for RDX than for HMX*.¹⁸ It has been suggested previously that the rate of thermal decomposition of HMX in the condensed phase is dominated by the rate at which the intermolecular forces allow the species to be separated.⁴ The lesser amount of intermolecular cohesion in RDX found in this work suggests that intermolecular forces have less influence on the rate of decomposition of RDX in the condensed phase than they do in HMX. It is known that RDX at its melting point decomposes an order of magnitude faster than HMX at its melting point.¹ We believe that this difference can be attributed to the diminished importance of the intermolecular forces in the thermal decomposition process of RDX.

Acknowledgment. We are grateful to the Air Force Office of Scientific Research, Air Force Systems Command for support of this work through AFOSR-80-0258. The contributions of Cheryl Landers (nee Ward) and James Baker to the computer graphics were most appreciated.

Registry No. RDX, 121-82-4.

(17) Kushida, T.; Benedek, G. B.; Bloembergen, N. *Phys. Rev.* **1956**, *104*, 1364.

(18) Consistent with this conclusion is the fact that RDX melts at 473 K while HMX melts at 543 K.